# Biogeography-Based Algorithm for High Voltage Electrode Surface Optimization of a Single-Phase GIS Bus Terminal

## Purushottam Padghan[1], Abhijit Mukherjee[1]

**Abstract:** A new method applying the biogeography-based optimization (BBO) technique is presented for the optimization of high voltage electrode surfaces. The aim is to obtain the optimization of the electrode shape in order to achieve a uniform field distribution along the surface of the electrode and maintain maximum field stress at minimum value. The principle of the developed optimization technique is described with an axi-symmetric single-phase GIS bus terminal electrode considered as a quarter-ellipse. In this scheme different aspects of the optimization technique are compared by means of semi-infinite line charges and ring charges to compute the electric field with the charge simulation method (CSM). The new Biogeography Based optimized approach helps in achieving a uniform field distribution with a minimum electric stress on the electrode surface and a minimum deviation angle for the otherwise normal stress vector, holding the assignment factor within the assigned range. The deviation angle is the more sensitive indicator of the simulation accuracy .The assignment factor has an impact on simulation accuracy. The combined BBO/CSM algorithm is capable of finding a better-quality solution, better accuracy, better convergence characteristics and computational efficiency.

**Keywords:** Biogeography-based optimization, Charge simulation method, Semi-infinite line charges, Ring charges, Deviation angle, Assignment factor.

## 1    Introduction

The optimization of the electrode contour in the high voltage field can be done by various techniques. Each has its own merits and limitations. Proper design of high voltage electrodes or any high voltage device requires a comprehensive knowledge of the electric field distribution. The field distribution along the contour should preferably be uniform and the maximum field stress along the contour should be within a set value. Various electric field computing methods have been used previously to optimize the electrode surface. Takuma and Kawamoto [1] proposed a method based on sequential quadratic programming that corresponds to an extended quasi-Newton method.

---
[1]Department of Electrical Engineering, Jadavpur University, Kolkata-32, West Bengal, India;
 E-mails: pnpadghan1066@gmail.com, abhimukh2001@yahoo.co.uk

The electric field was calculated using CSM together with spline-function smoothing, whereby priority was given to uniform field distribution. S.Chakravorti et al. [2] presented a new technique based on a neural network for optimization of electrode contours. P.K.Mukherjee et al. [3] employed an artificial neural network, the so-called resilient propagation algorithm. Here also CSM was used for preparation of the training sets as well as for checking the test outputs from the network. H.Okubo et al. [4], too, calculated an optimum contour with an electric field optimization method based on a neural network. Neural network-based applications, however, impose a huge computational burden and a certain amount of training is required to achieve the desired accuracy. A.Chatterjee et al. [5] developed a self-organizing fuzzy interface system for electrode optimization, but there was less uniformity in the electric field stress. Abdel Salam et al. [6] presented a genetic algorithm for optimization of high voltage electrode surfaces where different fitness functions were proposed and tested. Statistical analysis of the different solutions were carried out which revealed that the computed standard deviation was more.

In most of the previous work, a statistical approach is considered for the sake of simulation accuracy. Yet if the same analysis controls the deviation angle and assignment factor the result is more authentic. When CSM is used to compute the electric field then, at a selected number of contour points, fictitious charges are placed in such a way that there effect is required to satisfy the boundary conditions. In such cases, for better simulation, measurement of the deviation angle between the normal and the computed stress vector on the electrode surface is more effective than the statistical analysis [13]. The deviation angle is defined as the angular deviation of the electric stress vector at the control point on the electrode surface from the direction of the normal to its surface at that point. This deviation angle is the main indicator of simulation accuracy. The simulation accuracy in the CSM depends upon the type and number of fictitious charges as well as the locations of fictitious charges and contour points. These different parameters are co-related by the 'assignment factor'. The assignment factor is defined as the ratio of the distance between two successive contour points to the distance between a contour point and the corresponding charge. The deviation angle is a sensitive indicator which is applied when ring charges are used for simulation. By keeping the deviation angle to a minimum and the assignment factor in the set range, simulation accuracy is far better and more accurate than the statistical approach.

As some methods do not meet both of these requirements, it is therefore necessary to employ the most effective optimization method by simplifying the formulation and implementation of the problem. The present paper describes a new method based on the biogeography-based optimization (BBO) technique for the optimization of high voltage electrode surfaces.

## 2    Biogeography-Based Optimization

A BBO algorithm has certain unique features which overcome several demerits of the conventional methods [7, 14]. In the engineering field biogeography is used similarly to genetic algorithms, neural networks, fuzzy logic, particle swarm optimization, evolutionary algorithms and other types of computer intelligence.

Biogeography is the study of the geographical distribution of biological organisms and is represented by mathematical models. Mathematical models of biogeography help to reveal the migration of species from one habitat to another. These models also describe how new species arise and how species become extinct. A habitat is any island (area) that is geographically isolated from other islands [7]. The more generic term 'habitat' is used rather than the term 'island'. High habitat suitability index (HSI) areas make good residences for biological species. HIS variables are dependent variables. Factors such as rainfall, diversity of vegetation, diversity of topographic features, land area and temperature are the features which correlate with the HSI. The variables that characterize habitability are called suitability index variables (SIVs) [7]. SIVs are independent variables of habitat.

High HSI habitats are more static in their species distribution than low HSI habitats [7] because they have a low species immigration rate and are saturated with species. High species emigration rate habitats offer species many chances to emigrate to adjacent habitats. Low HSI habitats have a low species emigration rate but because of their sparse population have a high immigration species rate. This immigration of new species improves low HSI habitats, because its biological diversity is relative to the suitability of a habitat. Low HSI habitats are more active in their species dispersion than high HSI habitats. Poor solutions can evolve into better solutions by accepting new features. At the same time high HSI solutions tend to share their features with low HSI solutions. Because of this sharing feature the quality of low HSI solutions improves and this new approach to problem-solving is known as biogeography-based optimization.

The immigration rate $\lambda$ and the emigration rate $\mu$ are functions of the number of species in the habitat [7]. Fig. 1 shows the species model of a single habitat based on the theory of biogeography where straight line curves are considered. In Fig. 1, with regard to the immigration curve, the maximum possible immigration rate I occurs when there are zero species in the habitat. As the number of species increases, some species are able to benefit from immigration to the habitat and thus the immigration rate decreases.

Habitat can support $S_{max}$ maximum number of species, whereby the immigration rate becomes zero. On the other hand, the emigration rate is zero when there are no species in the habitat. As the number of species increases, the

habitat becomes crowded; some species are able to explore other possible habitats, and thus the emigration rate increases. When the habitat supports the largest possible number of species, the emigration rate E becomes maximal. The point S$_o$ has an equal number of species for which the rates λ and μ are equal.
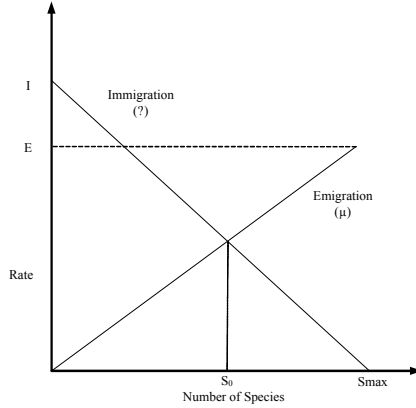


**Fig. 1 –** *Species model of a single habitat.*

If $P_s$ is the probability for S species in a habitat then for the small change in the interval we have the following equation:

$$P_s(t + \Delta t) = P_s(t)(1 - \lambda_s \Delta t - \mu_s \Delta t) + P_{s-1}\lambda_{s-1}\Delta t + P_{s+1}\mu_{s+1}\Delta t . \qquad (1)$$

In (1) $\lambda_s$ and $\mu_s$ are the immigration and emigration rates for $S$ species in the habitat. To keep $S$ species at time $(t + \Delta t)$ one of the following conditions must obtain:

1. there were $S$ species at time t, and no immigration or emigration occurred between t and $(t + \Delta t)$;
2. there were $(S - 1)$ species at time t, and one species immigrated;
3. there were $(S + 1)$ species at time t, and one species emigrated.

Assuming $\Delta t$ is very small and taking the limit of (1) as $\Delta t \rightarrow 0$ gives [7]:

$$P_s = \begin{cases} -(\lambda_s + \mu_s)P_s + \mu_{s+1}P_{s+1}, & S = 0, \\ -(\lambda_s + \mu_s)P_s + \lambda_{s-1}P_{s-1} + \mu_{s+1}P_{s+1}, & 1 \leq S \leq S_{max} - 1, \\ -(\lambda_s + \mu_s)P_s + \lambda_{s-1}P_{s-1}, & S = S_{max}. \end{cases} \qquad (2)$$

For convenience, $P_s$ equations can be formatted into the single matrix equation

$$\overline{P} = AP , \qquad (3)$$

where matrix $A$ is given (for $S = 0, \ldots, n$ ) as [7]:

$$A =$$
$$\begin{bmatrix} -(\lambda_0 + \mu_0) & \mu_1 & 0 & \cdots & 0 \\ \lambda_0 & -(\lambda_1 + \mu_1) & \mu_2 & \cdots & \vdots \\ \vdots & \vdots & \ddots & \vdots & \vdots \\ \vdots & \cdots & \lambda_{n-2} & -(\lambda_{n-1} + \mu_{n-1}) & \mu_n \\ 0 & \cdots & 0 & \lambda_{n-1} & -(\lambda_n + \mu_n) \end{bmatrix}. \quad (4)$$

For the straight-line curves shown in Fig. 1, the immigration and emigration rates are defined as [7]:

$$\mu_k = \frac{E_k}{n}, \quad n = S_{max}, \quad (5)$$

$$\lambda_k = I\left(1 - \frac{k}{n}\right). \quad (6)$$

In some special cases (for $\mu_k + \lambda_k = E$), (5) and (6) can be modified to compute the $\lambda$ and $\mu$ so that in (4) the elements of the matrix change [15]. With the help of Observation1 and Conjecture1 [7], an eigenvalue equation can be used to find the unknown vector v. Such eigenvalues are used to compute the steady-state value for the probability of each species. This probability is given by [7]:

$$P_{(\infty)} = \frac{v}{\sum_{i=1}^{n+1} v_i}, \quad (7)$$

where

$$v = \begin{bmatrix} v_1 & \cdots & v_{n+1} \end{bmatrix}^T,$$

$$v_i = \begin{cases} \dfrac{n!}{(n-1-i)!(i-1)!}, & (i = 1, \ldots, i') \\ v_{n+2-i}, & (i = i'+1, \ldots, n+1) \end{cases} \quad (8)$$

where

$$i' = \begin{cases} \leq (n+1)/2, \text{ or} \\ \text{ceil}((n+1)/2). \end{cases}$$

In mathematical models, each individual solution is a vector of integers (discrete version) which is initialized randomly and is applied to the problem's dependent functions. BBO algorithms have been successfully implemented to solve various problems. BBO is mainly based on two concepts: migration and mutation.

## 2.1 Migration

Migration can occur between any two habitats depending upon the emigration and immigration rates. Each integer in the solution vector is considered to be a suitability index variable (SIV). There is a method of assessing the goodness of the solutions. Good solutions have high HSI and poor solutions have low HSI. HSI is analogous with 'fitness' in other population-based optimization algorithms. High HSI solutions represent habitats with many species, and low HSI solutions represent habitats with few species. The use of emigration and immigration rates helps each solution to probabilistically share information between habitats. If a given solution is selected to be modified, then we use its immigration rate to probabilistically decide whether or not to modify each suitability index variable in that solution. If a given SIV in a given solution is selected to be modified, then we use the emigration rates of the other solutions to probabilistically decide which of the solutions should migrate a randomly selected SIV to that solution [7]. The difference in the global recombination approach of evolutionary strategies and the migration of BBO is that the former approach is used to create a new solution whereas the latter approach is used to change the existing solution.

## 2.2 Mutation

In BBO, when the change in habitat's HSI occurs suddenly the event is represented by the mutation of the SIV, and species count probabilities are used to determine mutation rates. The species count probability can be calculated. Each population member has an associated probability which indicates the likelihood that it exists as a solution for a given problem. If the probability of a given solution is very low, then that solution is likely to mutate to some other solution. Similarly, if the probability of some other solution is high, then that solution has very little chance to mutate [7]. Therefore, very high HSI solutions and very low HSI solutions are equally improbable in terms of mutation; i.e., they have fewer chances to produce more improved SIVs in the later stage. But Medium HSI solutions, however, have better chances to create much better solutions after mutation. The mutation rate of each set of solutions can be calculated in terms of species count probability. The mutation rate $m$ is defined as [7]:

$$m(s) = m_{\max} \left( \frac{1 - P_s}{P_{\max}} \right). \qquad (9)$$

Here $m_{\max}$ is a user-defined parameter. This mutation scheme tends to increase diversity among populations. Without this modification, the highly probable solutions tend to be more dominant in the population. This mutation approach makes both low and high HSI solutions likely to mutate, which means both types of solution improve on their earlier values. An elitism approach is

used to save the features of the habitat that has the best solution in the BBO process, so even if mutation ruins its HSI, it has been saved it and can be retrieved if needed [7]. Therefore, the mutation operation is a high-risk process. It is normally applied to both poor and good solutions. Since medium-quality solutions are in the improvement stage, it is better not to apply mutation to them. The implemented mutation mechanism is problem-dependent. In the present work mutation of a selected solution is performed simply by replacing it with a randomly generated new solution set.

### 2.3 BBO algorithm

The BBO algorithm involves the following steps in sequence.

1. Initialize a set of solutions to a problem.

2. Compute the fitness (HSI) of each solution.

3. Compute the number of species, and the immigration and emigration rates of each solution.

4. Modify habitats (migration) based on immigration and emigration rates.

5. Compute mutation based on probability.

6. If necessary, implement elitism.

7. Repeat steps 2 to 6 for a number of iterations.

Feasibility as a problem solution should be verified after each habitat modification. The objective of the present work is to use a BBO algorithm for the optimization of electric field distribution along a high voltage electrode surface. For flexibility, the electrode contour selected is a quarter-ellipse. A practical example of a single-phase GIS bus with an axi-symmetric system is presented [6]. A BBO algorithm model is developed to determine the parameters which define the shape of the electrode contour through the maximization of the relevant fitness function. The fitness function employed in the present work is the square root of the accumulated squared field deviations from a pre-specified maximum field value [6]. The proposed method offers effectiveness and accuracy with better convergence characteristics and computational efficiency.

## 3   Preparations and Simulation Technique

Fig. 2 shows a typical GIS bus termination. It is an axi-symmetric system [6]. The radii r and R of the HV conductor and the grounded external cylinder are fixed. The height H is also specified. The major part of contour G to be optimized is a quarter-ellipse, and semi-axes $x_1$ and $x_2$ and $x_3 = 1 - x_2$ can be computed. The contour between the central axis and the beginning of the quarter ellipse is taken as a disc of radius $x_2$ which is perpendicular to the

central axis, $R = 2.75$, $r = 1$ and $H = 1.5$ units. The voltage of the conductor is assumed to be unity. $N$ is a Neumann plane on which the normal component of the flux density is zero and equipotential lines are all perpendicular to $N$.
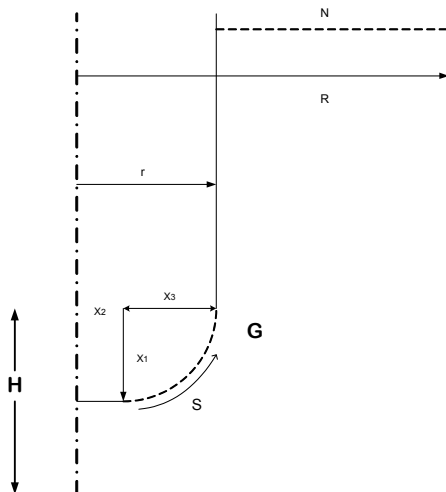


**Fig. 2** – *Axi-symmetric single-phase GIS bus termination.*

Under favourable conditions the charge simulation method (CSM) [8 – 10] is used for field computation. This method has many features, such as high calculation accuracy, applicability to electrodes with round surfaces, easy setting of boundary conditions, reduced number of input data and feasibility in analysis. The CSM is an integral equation technique which makes use of mathematical linearity and expresses the Laplace equation as a summation of a particular solution owed to a set of known discrete fictitious charges. The basic principle of the charge simulation method is very simple. According to the superposition principle

$$\Phi_i = \sum_{j=1}^{n} P_{ij}Q_j \,, \tag{10}$$

where $P_{ij}$ are the 'potential' coefficients which can be evaluated analytically for many types of charges by solving Laplace or Poisson equations.

For field estimation proper selection of suitable types of simulation charges [8 – 10] and their appropriate arrangement is a very important aspect of CSM [11, 12]. The inherent ability of CSM to simulate curved and rounded surfaces of electrodes or interfaces of different dielectric materials in a rather simple fashion makes it a very appropriate method. In CSM fictitious charges are required to satisfy the boundary conditions only at a selected number of contour

points. To determine the simulation accuracy different criteria can be used. The potential error which is the difference between the known potential of the electrode and the computed potential at the control point should be minimal. This potential error is usually in the order of $10^{-3}$ [10]. The error in the electric stress is usually higher than the potential error. This error in the electric stress is effectively measured by the deviation angle which is the most sensitive indicator of simulation accuracy, and is used when ring charges are used for the simulation. If the deviation angle is in the range of $\pm 3$ degrees, then there is a very small difference between the mean value of electric stress and the maximum electric stress which results in more uniform field distribution along the electrode surface. The assignment factor considerably affects the simulation accuracy. H. Singer et al. suggested that the assignment factor should lie between 1.0 and 2.0 [8]. Other researchers have suggested that this factor gives satisfactory results when it lies between 0.7 and 1.5.

In order to simulate the GIS electrode, field computations are analysed with two types of charges separately: first, semi-infinite line charges and, second, ring charges. The former charges are arranged along the central axis [6]. Two parameters $t_1$ and $t_2$ are used to determine both the initial location and the axial distribution of the charges in order to obtain accurate potentials on the boundaries by using a suitable error function. The first parameter $t_1$ determines the location of the first charge which is usually located close to the centre of the ellipse. The axial distribution of the charges in an exponential manner is controlled by the parameter $t_2$.

An exponential function given by (11) is used [6]

$$e_{(i)} = e_{(i-1)} + t_3 \exp\left(t_2 \, \frac{i}{n}\right), \quad i = 2{:}n \,, \tag{11}$$

where $e_{(i)}$ is the axial location of the ith charge, and $e_{(1)}$ is the axial location of the first charge which is equal to $t_1$. The parameter $t_2$ is a real value equal to or greater than zero. The parameter $t_3$ is the adjustment factor for the location of any other charge. Appropriate values of $t_1$ and $t_2$ are found when the fitness function reaches a set value. The location of the Neumann plane $N$ is taken to equal approximately $3H$ so that the value of the fitness function is within the assigned value [6].

In the second case when ring charges are used for field computation, more prominent simulation takes place. These types of charges are more suitable for the present electrode geometry [11, 12]. The ring charges are uniformly located along the central axis. The radius of any ring charge is determined by:

$$r_{(j)} = fa\left(\frac{D(b^2 - (Z_{(j)} - H)^2)}{g}\right)^{1/2} + r_1, \quad j = 2{:}m \,, \tag{12}$$

where $fa = a/b$, $j$ is the number of contour points on the electrode surface, $a$ and $b$ are the major and minor axis of the ellipse respectively, $D$ is the distance between the point charge and contour along central axis, $g$ is the distance between the ground and contour along central axis, $z$ is the location of ring charges, $H$ is the height and $r_1$ is the co-ordinate of the first charge. The location of the Neumann plane $N$ is the same as in the first case. The first charge is considered as a point charge and the rest of the charges are ring charges. If the proper values of $fa$ are selected, the fitness function will satisfy the required objective of controlling the measuring indicators well within the range.

Because of the different stress distributions for the GIS bus termination, the field distribution along the electrode surface is generally non-uniform and may contain more than one peak. The BBO technique is proposed for the solution of such problems. The parameters $x_1$ and $x_2$ are the habitats and the BBO algorithm searches for their optimum values through a properly designed fitness function to achieve uniform field distribution along the electrode contour and to maintain the maximum field stress at a minimum value. In the present work, the proposed BBO/CSM algorithm requires the following steps.

1. Using a few CSM trials determine the domain for the optimum dimensions of $x_1$ and $x_2$ for semi-infinite line charges and ring charges separately.

2. Enter these ranges in the BBO algorithm as inputs to generate initial random values of $x_1$ and $x_2$ in each case separately.

3. For each call to the CSM routine by BBO algorithm, for a given value of $x_1$ and $x_2$, unknown charges are determined:

    (a) First, for the appropriate values of $t_1$ and $t_2$, semi-infinite line charges are determined locally within the CSM routine and,

    (b) Second, for the appropriate ratio of $fa$ ring charges are determined locally within the CSM routine.

4   The CSM will then produce the field distribution along the electrode surface using both charges separately under these conditions:
    (a) minimum standard deviation using semi-infinite line charges and
    (b) minimum deviation angle and the assigned assignment factor using ring charges.

5   Determine the best solution with minimum error during this iteration in each case separately.

6   Update the location of each solution (location of its simulation charges) depending on the location of the best solution.

7   The BBO algorithm will evaluate a fitness function and modify $x_1$ and $x_2$ accordingly in both types of charges separately.

8    Repeat steps 3 to 7 for a set number of generations in each case.

The expression for the proposed fitness function [6] is:

$$U_1 = \frac{1}{\left(1 + U_a\right)}, \tag{13}$$

where $U_a$ is given by

$$U_a = \left( \sum_{j=1}^{m_1} \left(E_j - E_1\right)^2 \right)^{1/2}, \tag{14}$$

where $E_j$ is the electric field at point $j$ on the elliptic part of the electrode, $m_1$ is the number of check points on that part, and $E_1$ is the minimum value of the maximum electric field. The value of $E_1$, within the domain of $x_1$ and $x_2$, is determined by the BBO algorithm. The same algorithm procedures as those described are used, with an alternate fitness function $U_b$, which takes the form:

$$U_b = \frac{1}{\left(1 + E_{\max}\right)}, \tag{15}$$

where, for a given $x_1$ and $x_2$, $E_{\max}$ is the maximum electric field value on the contour part of the electrode surface. The minimum value is the required field stress $E_1$ in (14) and is computed by applying the BBO algorithm to (15). The problem is now to determine the optimum values of the parameters $x_1$ and $x_2$ subject to the satisfaction of the fitness function given by (13). In the execution process, first compute $E_1$ and then determine the optimum values of $x_1$ and $x_2$.

## 4    Simulation Results

As shown in Fig. 2 an axi-symmetric single-phase GIS bus termination is considered [6]. In the first case where the semi-infinite line charges are used the number of simulating charges is 11. The first is a point charge and the remaining 10 are semi-infinite line charges. The habitat modification probability Pm is 1.0 and the mutation rate is 0.5. The number of generations, Ng, used in the BBO pattern is 50 and the population size Np is 10. The parameters $x_1$ and $x_2$ are randomly generated well within the domain. The parameter $x_1$ is selected to lie between 0.6 and 0.75, whereas $x_2$ varies between 0.01 and 0.2. The CSM parameters, $t_1$ and $t_2$, are selected to vary between –0.1 and +0.1 and 1.0 to 3.0, respectively. The fitness function to be maximized is given by (13). The minimum value of the maximum field stress, $E_1$, within the considered domain is found to be 1.70, 0.5 less than in the previous result [6].

In the second case simulation is run by using 20 ring charges. The first is a point charge and the remaining 19 are ring charges which are located along the central axis. The parameter *fa* is selected to lie between 1.2 and 1.8. The

minimum value of the maximum field stress $E_1$ within the considered domain is found to be 1.35. This is a considerable change in value. The remaining parameters and conditions required for ring charges are the same as those considered in semi-infinite line charges. To know the details of the analysis various fitness functions are tested [6]. Eq. (13) was the first and the second fitness function is based on the average of the electric field values, $E_a$, at the contour points and stated as:

$$U_2 = \frac{1}{\mathrm{abs}\left(E_a - E_1\right)} .$$

(16)

The third fitness function verified is given by:

$$U_3 = \frac{1}{\left[\mathrm{abs}\left(E_h - E_l\right)/2 - E_1\right]},$$

(17)

where $E_h$ is the highest field value of the distribution and $E_l$ is its lowest value.

The results for the electric field distribution along the electrode contour for the various fitness functions are shown in Fig. 3 by semi-infinite line charges. It can be seen that field distribution obtained using (13) is more uniform than that of (16) and (17). In order to demonstrate the generality of the method, values of the maximum stress $E_1$, other than its minimum value on the electrode contour, are considered. For this purpose, three arbitrary values of $E_1$ are tested and their field distribution is shown in Fig. 4.
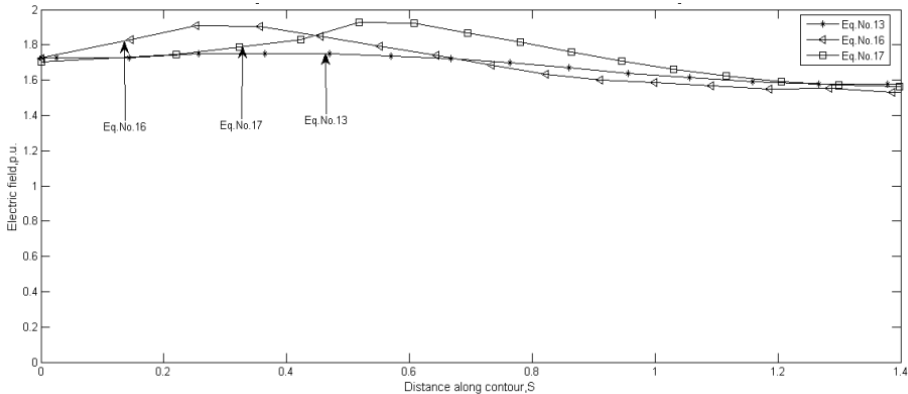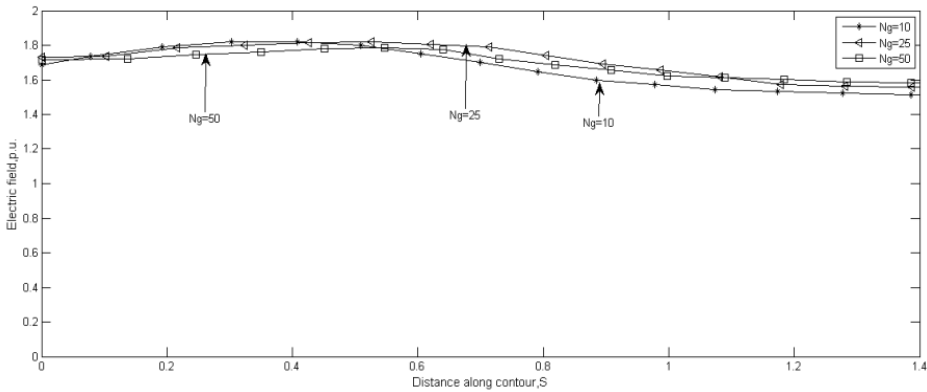


**Fig. 3** – *Field distribution for different fitness functions using semi-infinite line charges.*

For each value of $E_1$ the algorithm is required to produce a uniform field distribution along the electrode surface while keeping the maximum field stress of the distribution at the required assigned value. Fig. 5 shows that for semi-infinite line charges, as the number of generations increases, the field distribution becomes more and more uniform and its mean value approaches the required maximum stress $E_1$.
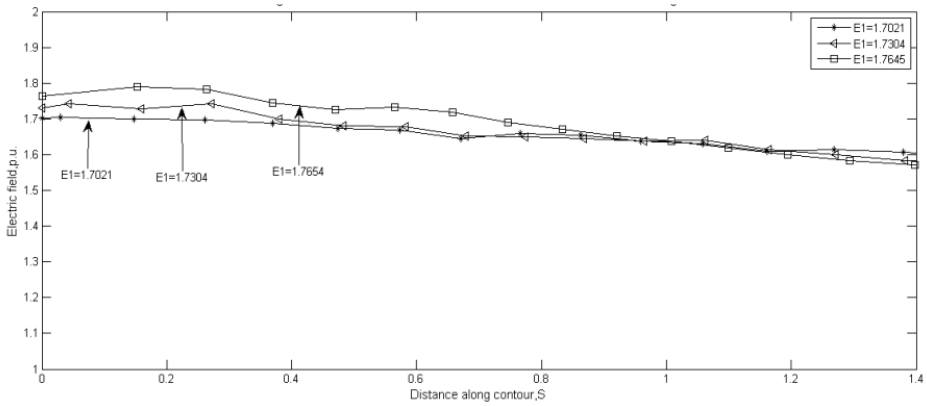
**Fig. 4** – *Field distribution for different values of $E_1$ using semi-infinite line charges.*



**Fig. 5** – *Convergence of the field distribution at different numbers of generations for semi-infinite line charges.*
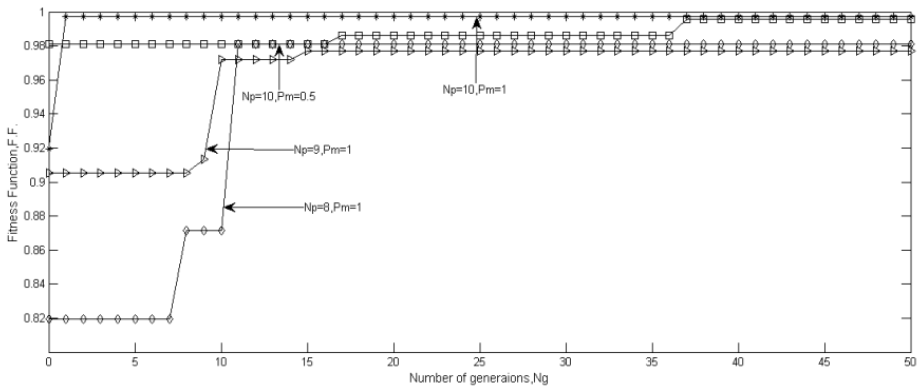


**Fig. 6** – *Convergence of the fitness functions for different values of $N_p$ and $P_m$ using semi-infinite line charges.*

225

In Fig. 6 the effect of the various parameters of BBO such as population size $N_p$ and the modification probability $P_m$ are analysed. When $N_p = 10$ and $P_m = 1$, the fitness function reaches its highest value and convergence occurs at below 50 generations.

**Table 1** expresses the statistical data for the different fitness functions and for different values of the required maximum stress $E_1$ for semi-infinite line charges. This shows that the fitness function of (13) is better at realizing the required objectives than the other two functions. The standard deviation which is a measure of uniformity is well within 10% for the considered cases. Compared with previous results [6] the present results are better, with a decrease in maximum field stress from 1.75 to 1.70 and consequently more uniform distribution of the electric field. For each fitness function the maximum stress as well as the standard deviation is considerably reduced. This shows that the present technique offers greater accuracy and requires fewer than 50 generations for better convergence.

**Table 1**
*Results for different fitness functions and for different values*
*of the required maximum stress $E_1$ for semi-infinite line charges.*

| Description | | Maximum Stress [p.u.] | Mean Stress [p.u.] | Standard Deviation [%] | $x_1$ | $x_2$ |
|---|---|---|---|---|---|---|
| Fitness Function | Eq. (4) | 1.7521 | 1.6780 | 6.1 | 0.6902 | 0.0224 |
| | Eq. (7) | 1.9109 | 1.6606 | 12.71 | 0.7222 | 0.1058 |
| | Eq. (8) | 1.9272 | 1.7021 | 11.55 | 0.7247 | 0.0653 |
| Required Stress $E_1$ [p.u.] | 1.70 | 1.7052 | 1.6251 | 6.14 | 0.7195 | 0.0146 |
| | 1.74 | 1.7423 | 1.6261 | 7.99 | 0.7125 | 0.0176 |
| | 1.78 | 1.7521 | 1.6780 | 9.23 | 0.6539 | 0.0640 |

When semi-infinite line charges are used for simulation it is very difficult to keep the assignment factor and deviation angle in the correct range to maintain the symmetry about the central axis. Assignment factor and deviation angle are the main indicators which measure the accuracy of electric stress. The required goal of keeping the field at minimum value and distributing it uniformly is achieved by the BBO algorithm with better convergence and with more accuracy using semi-infinite line charges than other methods [6].

In our second case, semi-infinite line charges are replaced by ring charges to optimize the electrode surface. The field distribution for different fitness functions is shown in Fig. 7. The value $E_1$ within the considered domain is considerably reduced from 1.70 in the case of semi-infinite line charges to 1.35 in the case of ring charges. For all three fitness functions the field distribution along the electrode contour is uniform but it is more pronounced in (13). The
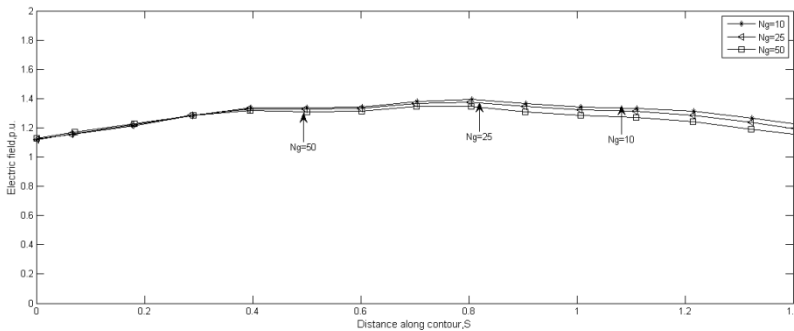
variation of $E_1$ which is helpful for the design of high voltage electrode surfaces is shown in Fig. 8.
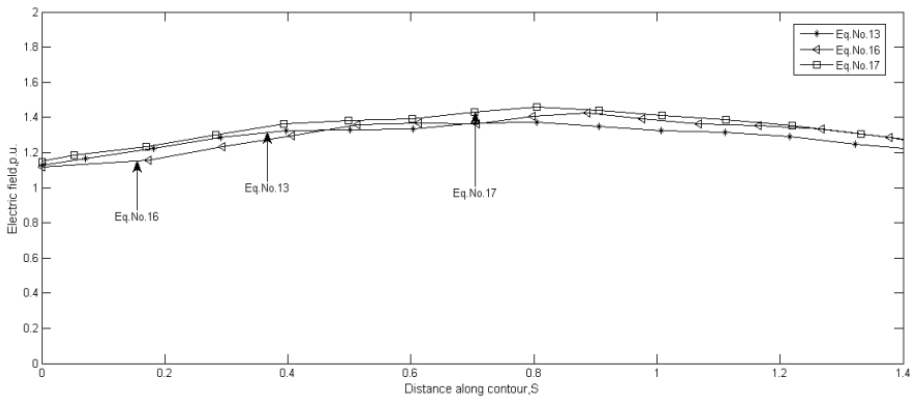


**Fig. 7** – *Field distribution for different fitness functions using ring charges.*
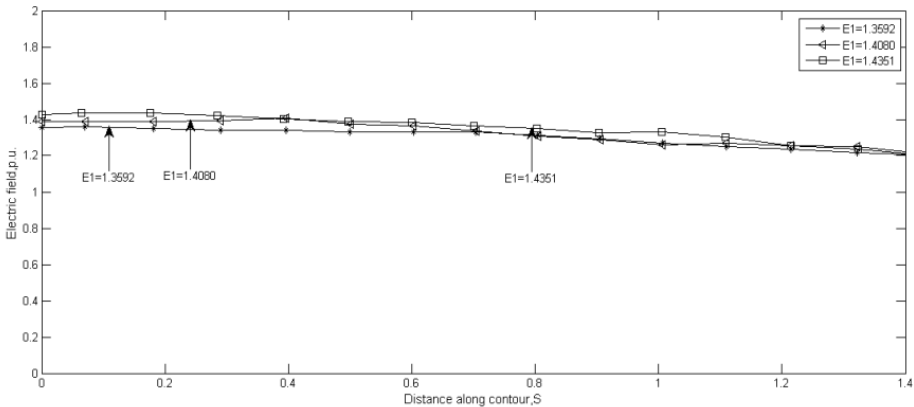


**Fig. 8** – *Field distribution for different values of $E_1$ using ring charges.*



**Fig. 9** – *Convergence of the field distribution at different numbers of generations, $N_g$, for ring charges.*

227

Fig. 9 indicates that for ring charges, as the number of generations increases, the field distribution becomes more uniform and its mean value approaches $E_1$.

The effect of the various parameters of BBO such as the population size $N_p$ and the modification probability $P_m$ is analysed and shown in Fig. 10 for ring charges. When $N_p = 10$ and $P_m = 1$ the fitness function reaches its highest value and convergence occurs at fewer than 50 generations.
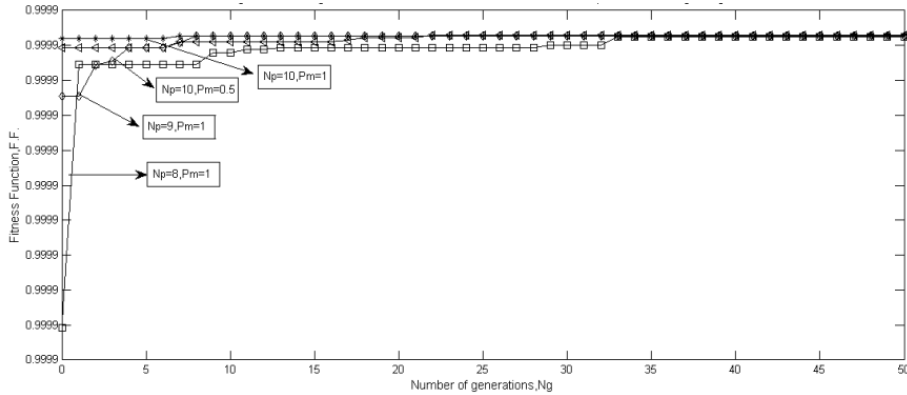


**Fig. 10** – *Convergence of the fitness functions for different values of $N_p$ and $P_m$ using ring charges.*

**Table 2**

*Results for different fitness functions and for different values of the required maximum stress $E_1$ for ring charges.*

| Description | | Max. Stress [p.u.] | Mean Stress [p.u.] | Standard Deviation [%] | Max. Deviation Angle [deg.] | $x_1$ | $x_2$ |
|---|---|---|---|---|---|---|---|
| Fitness Function | Eq. (4) | 1.3754 | 1.2504 | 8.67 | 2.8887 | 0.7123 | 0.0593 |
| | Eq. (7) | 1.4272 | 1.2683 | 10.74 | 3.0120 | 0.6334 | 0.0199 |
| | Eq. (8) | 1.4591 | 1.2949 | 10.88 | -3.0603 | 0.7186 | 0.0924 |
| Required Stress $E_1$ [p.u.] | 1.35 | 1.3592 | 1.2707 | 7.06 | 2.9682 | 0.7188 | 0.1585 |
| | 1.40 | 1.4080 | 1.2824 | 9.40 | -3.0870 | 0.7183 | 0.1593 |
| | 1.43 | 1.4351 | 1.3088 | 9.69 | -3.1133 | 0.7210 | 0.1489 |

**Table 2** presents the results for the different fitness functions and for different values of the required maximum stress $E_1$ using ring charges. The maximum deviation angle for field distribution using (13) is smaller than that of (16) and (17) and helps to obtain more uniform field distribution along the contour. For (13) the maximum deviation angle 2.8887 is well below the assigned value and leads with a very smooth curve, as shown in Fig. 7. The field distribution for different values of $E_1$ is more linear in the case of ring charges, as shown in Fig. 8. Comparison shows that results obtained using ring charges are far better than those obtained for semi-infinite line charges.

The BBO method encourages the overall optimization of the GIS bus termination by using both types of charges: first semi-infinite lines charges and then ring charges. This is achieved by the determination of the optimum dimensions of $x_1$, $x_2$, and $H$. For semi-infinite line charges the electrode configuration, the domain for the parameters $x_1$, $x_2$, the value of $E_1 = 1.7$ and the fitness function given by (13) are the same as before. The value of $H$ is assumed to lie between 1.4 and 1.5. The rest of the BBO parameters remain same. After analysis the maximum, mean and standard deviations of the field distribution are 1.8043, 1.7011 and 6.03% respectively. The deviation of the maximum stress from the obtained value is 6.135%. The optimized parameters $x_1$, $x_2$, and H are 0.6336, 0.1861 and 1.46 respectively for semi-infinite line charges. Fig. 11 shows the overall optimized field distribution along the electrode contour for semi-infinite line charges.
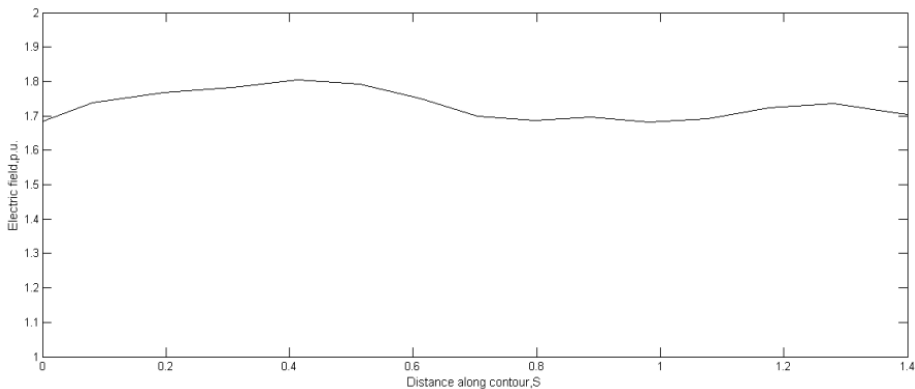


**Fig. 11** – *An overall optimized field distribution along the electrode contour for semi-infinite line charges.*

In the second case, for ring charges the electrode configuration, the domain for the parameters $x_1$, $x_2$, the value of $E_1 = 1.35$ and the fitness function given by (13) are the same as before. The value of $H$ is assumed to lie between 1.45 and 1.5. The BBO parameters are same as before. After analysis the maximum,

mean and standard deviations of the field distribution are 1.4120, 1.3421 and 5.27% respectively. The deviation of the maximum stress from the required value is 4.593% and the optimized parameters $x_1$, $x_2$, and $H$ are 0.7188, 0.1585 and 1.49 respectively. The maximum deviation angle is 2.7853. Fig. 12 shows the overall optimized field distribution along the electrode contour for ring charges, which is more uniform than for semi-infinite line charges.
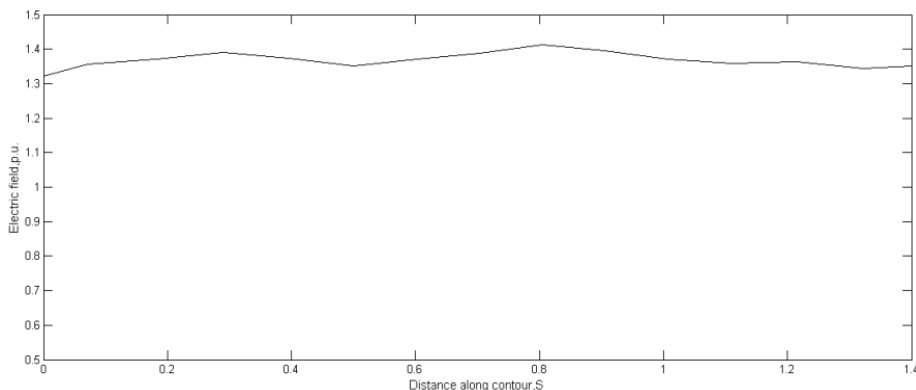


**Fig. 12** – *An overall optimized field distribution along the electrode contour for ring charges.*

## 5    Conclusion

A new biogeography-based optimization technique is presented for the optimization of high voltage electrode surfaces. The main goal of keeping uniform field distribution along the contour and maintaining maximum field stress at minimum value is achieved. Compared with previous results [6] the minimum value of the maximum field stress, $E_1$, within the considered domain is reduced from 1.75 to 1.70 when semi-infinite line charges are used. Observations show that the standard deviation reduces considerably keeping the uniform field along the surface of the electrode. Convergence of the fitness function occurs at fewer than 50 generations.

What transpires from the present work is that, for typical electrode geometry, if ring charges are used for the simulation the results are much better as compare to the previous results in all respects. The minimum value of the highest field stress $E_1$ anywhere on the electrode surface is reduced from 1.75 to 1.35. The assignment factor lies between 0.9 and 1.8. The deviation angle is in the range of $\pm 3$ degrees. This shows that the simulation accuracy is near to its best possible level. Convergence of all the three fitness functions occurs at fewer than 50 generations. The method is used to demonstrate the overall optimization of the GIS bus terminus using both semi-infinite line charges and ring charges. It is found that for electrode configuration, applying BBO to

optimize the surface of the electrode and simulation by ring charges is a very effective option. The accuracy measures of electric stress, like deviation angle and assignment factor are within assigned values and the overall optimized field distribution along the electrode contour is much uniform.

# 6   References

[1]   T. Kawamoto, T. Takuma, H. Yasuda, Y. Ohtsuka: Optimization of Conductor Shapes by the SQP, 1st Lecturer Meeting, JSCES, A-16-4, 1997.

[2]   S. Chakravorti, P.K. Mukherjee: Application of Artificial Neural Networks for Optimization of Electrode Contours, IEEE Transactions on Dielectrics and Electrical Insulation, Vol. 1 No. 2, April 1994, pp. 254 – 264.

[3]   P.K. Mukherjee, C. Trintis, H. Steinbigler: Optimization of HV Electrode Systems by Neural Networks using a New Learning Method, IEEE Transactions on Dielectrics and Electrical Insulation, Vol. 3, No. 6, Dec. 1996, pp. 737 – 742.

[4]   H. Okubo, T. Otsuka, K. Kato, N. Hayakawa, M. Hikita: Electric Field Optimization of High Voltage Electrode Based on Neural Network, IEEE Transactions on Power Systems, Vol. 12,  No. 4, Nov. 1997, pp. 1413 – 1418.

[5]   A. Chatterjee, A. Rakshit, P.K. Mukherjee: A Self-organizing Fuzzy Inference System for Electric Field Optimization of HV Electrode Systems, IEEE Transactions on Dielectrics and Electrical Insulation, Vol. 8 , No. 6, Dec. 2001, pp. 995 – 1002.

[6]   M.S. Abdel-Salam, M.M. Abouelsaad: A New Method for Optimization of High Voltage Electrode Surfaces using Genetic Algorithms, Alexandria Engineering Journal, Vol. 42, No. 2, 2003, pp. 201 – 208.

[7]   D. Simon: Biogeography-based optimization, IEEE Transactions on Evolutionary Computation, Vol. 12, No. 6, Dec. 2008, pp. 702 – 713.

[8]   H. Singer, H. Steinbigler, P. Weiss: A Charge Simulation Method for the Calculation of High Voltage Fields, IEEE Transactions on Power Apparatus and Systems, Vol. 93, No. 5, Sept. 1974, pp. 1660 – 1668.

[9]   N.H. Malik: A Review of the Charge Simulation Method and its Applications, IEEE Transactions on Electrical Insulation, Vol. 24 No. 1, Feb. 1989, pp. 3 – 20.

[10]  A. Yializis, E. Kuffel, P.H. Alexander: An Optimized Charge Simulation Method for the Calculation of High Voltage Fields, IEEE Transactions on Power Apparatus and Systems, Vol. 97, No. 6, Nov. 1978,  pp. 2434 – 2440.

[11]  S. Chakravorti, P.K. Mukherjee: Efficient Field Calculation in Three-core Belted Cable by Charge Simulation Using Complex Charges, IEEE Transactions on Electrical Insulation, Vol. 27, No. 6, Dec. 1992, pp. 1208 – 1212.

[12]  R. Nishimura, K. Nishimori, N. Ishihara: Determining the Arrangement of Fictitious Charges in Charge Simulation Method using Genetic Algorithms, Journal of Electrostatics, Vol. 49, No. 1-2, May 2000,  pp. 95 – 105.

[13]  E. Kufel, W.S. Zaengel, J. Kuffel: High Voltage Engineering: Fundamentals, Newnes, Oxford, UK, 2000.

[14]  D. Simon, R. Rarick, M. Ergezer, D. Du: Analytical and Numerical Comparisons of Biogeography-based Optimization and Genetic Algorithms, Information Sciences, Vol. 181, No. 7, April 2011, pp. 1224 – 1248.

[15]  H. Ma: An Analysis of the Equilibrium of Migration Models for Biogeography-based Optimization, Information Sciences, Vol. 180, No. 18, Sept. 2010, pp. 3444 – 3464.